Carbohydrate Polymers 82 (2010) 291–298

Contents lists available at ScienceDirect

Carbohydrate Polymers

journal homepage: www.elsevier.com/locate/carbpol

Study of the combined effect of both clay and glycerol plasticizer on the properties of chitosan films

Marino Lavorgna [a], Filomena Piscitelli [a,b], Pasqualina Mangiacapra [a], Giovanna G. Buonocore [a,*]

[a] National Research Council, Institute for Composite and Biomedical Materials, P.le E. Fermi, 1, 80155 Portici (Naples), Italy
[b] Department of Materials Engineering and Production, University of Naples Federico II, P.le Tecchio 80, 80125 Naples, Italy

ARTICLE INFO

Article history:
Received 12 February 2010
Received in revised form 9 April 2010
Accepted 20 April 2010
Available online 29 April 2010

Keywords:
Chitosan
Nanocomposite
Na-MMT
Glycerol

ABSTRACT

Chitosan-based nanocomposites at different sodium montmorillonite loadings, with and without glycerol as plasticizer, were produced by solution casting. The combined effect of glycerol and silicate clay on the thermal, mechanical and barrier properties of the obtained nanocomposites was investigated. Films containing 10% (wt/wt) of Na-MMT show, with respect to neat chitosan, reduced water permeability of about 30% and 50% and an increased tensile strength of about 120% and 25%, for films with and without glycerol, respectively. The improvement of barrier and mechanical properties was correlated both to the films nanostructure and to the interactions between chitosan, Na-MMT and glycerol. XRD results suggest that in films without glycerol, which exhibit the best barrier properties, the Na-MMT stacks lay with their platelets parallel to the casting surface. The nanocomposites obtained with addition of glycerol show the best mechanical properties due to the enhancement of chitosan intercalation in the silicate galleries.

1. Introduction

Polymers obtained from renewable sources, generally biodegradable under normal environmental conditions, can be a viable solution to the waste disposal of plastic food packaging materials, and, for this reason, have been widely investigated over the last several years. In order to compete with synthetic plastics, they should have comparable mechanical and/or barrier properties. This is especially difficult to achieve with respect to moisture barrier properties, because of the hydrophilic nature of most biopolymers which is in contrast with the hydrophobic nature of most synthetic polymers used in food packaging, typically polyolefins.

Chitosan is one of the most interesting biopolymers obtained from natural sources. As reported by Tual, Espuche, Escoubes, and Domard (2000), in addition to the biocompatibility characteristics, chitosan bacterio- and fungi-static properties are very useful for food preservation. It is a polysaccharide obtained by deacetylation of chitin. The degree of deacetylation (DDA) in chitin usually ranges from 5% to 15% and in chitosan from 70% to 95%. The degree of acetylation (DA) and the crystallinity of chitin molecules affect the solubility in common solvents. Reducing the acetylation level in chitosan ensures the presence of free amino groups, which can be easily protonated in acid environment, making chitosan soluble in aqueous acid solutions.

As for other biopolymers, many strategies have been explored to improve the barrier and mechanical properties of chitosan-based biodegradable packaging films. These include the addition of plasticizers such as glycerol which increase flexibility of the final product (Srinivasa, Ramesh, & Tharanathan, 2007). The addition of other biodegradable aliphatic polyesters, such as poly-caprolactone (PCL), poly(butylene succinate) (PBS), poly(lactic acid) (PLA), poly(butylene terephthalate adipate) (PBTA), and poly(butylene succinate adipate) (PBSA) (Correlo et al., 2005; Olabarrietaa, Forsstrom, Gedde, & Hedenqvist, 2001), has also been investigated to produce materials with properties intermediate between the two components. Other methods included the addition of layered silicates nanoparticles (e.g. sodium montmorillonite) to improve its end-use properties such as barrier and mechanical properties. Xu, Ren, and Hanna (2006), in fact, found that natural sodium montmorillonite increases thermal and mechanical properties of the chitosan nanocomposite. Gunster, Pestreli, Unlu, Atici, and Gungor (2007) found that both the structure of chitosan/Na-MMT nanocomposites and its thermal stability are strongly affected by the solvent-casting procedure used. Wang et al. (2005) have investigated the effect of both acetic acid (HAc) residue and the hydrogen bonds formed between chitosan and MMT on the nanocomposite properties. They showed that the residual HAc accelerates the thermal decomposition of chitosan and decreases its crystallinity level. More recently, Tang et al. (2009) have investigated the effect of using nanofillers with different dimensions, such as two-dimension clay platelets and one-dimension carbon nanotubes, on the properties of chitosan. They have obtained an improvement of thermal stability, mechanical and barrier properties of chitosan.

* Corresponding author. Tel.: +39 081 7758837; fax: +39 081 7758850.
E-mail address: gbuonoco@unina.it (G.G. Buonocore).

0144-8617/$ – see front matter © 2010 Elsevier Ltd. All rights reserved.
doi:10.1016/j.carbpol.2010.04.054

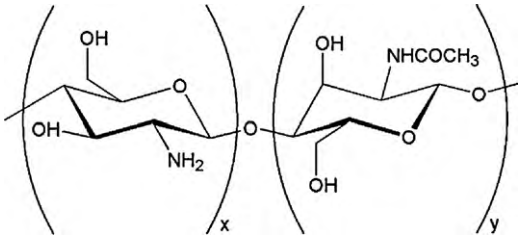

Scheme 1. Chitosan chemical structure.

Although several papers on chitosan–clay nanocomposites have appeared in the literature, there are no reported data on the studies of the combined effect of both clays and plasticizers on the end-use properties. Thus, the aim of this work is to analyze the role of glycerol in the solution-casting procedure for the achievement of chitosan/clay nanocomposite films. The interest in the use of glycerol is mainly due to the following factors: (i) glycerol, acting as plasticizer, reduces the intermolecular forces increasing the mobility of the biopolymer chains (Srinivasa et al., 2007); (ii) glycerol reduces the extent of edge–edge interactions (i.e. H-bonding interactions), between Na-MMT stacks making it possible to achieve a better dispersion of nanosized filler (Darder, Colilla, & Ruiz-Hitzky, 2003); (iii) glycerol can modify the ability of water to swell MMT in the aqueous solution, due to its ability to reduce the surface energy of aqueous solution (Shanmugharaj, Rhee, & Ryu, 2006). The interaction between solvents and clays controls the dispersion of the platelets and, as a consequence, it determines also the resulting properties of nanocomposites (Burgentzlè, Duchet, Gerard, Jupin, & Fillon, 2004).

In order to investigate the combined effect of glycerol and unmodified Na-MMT on the properties of chitosan-based nanocomposites, films containing different amount of clay and glycerol were prepared and characterized with particular regard to structural, thermal, mechanical and barrier properties.

2. Experimental

2.1. Materials

High molecular weight chitosan (CS) in powder form (310–375 kDa, with a deacetylation degree greater than 75%) was bought from Sigma–Aldrich (Italy). Its chemical structure is schematically shown in Scheme 1.

The pristine clay (Na^+-montmorillonite) was purchased from Southern Clay Products, Inc., TX. Glacial acetic acid (HAc) was obtained from Sigma–Aldrich (Italy) to produce acetic acid solutions. Glycerol obtained from Fluka (Italy) was used as plasticizer.

2.2. Preparation of chitosan nanocomposite films

Chitosan solution was prepared by dissolving 2 g of CS powder in 100 ml of aqueous acetic acid solution (1%, v/v), using a magnetic stirring plate at 90 °C and 150 rpm for 20 min and then cooled to room temperature. Nanocomposite samples were obtained by dispersing selected amounts of clay (3 and 10% (wt/wt) on solid CS) in 100 ml of 1% (v/v) aqueous acetic acid solution for 1 h at room temperature. This dispersion was added to the CS solution, stirred for 1 h at room temperature and then for 30 min at 25 °C in an ultrasonic bath. The dispersion was then poured onto glass discs (diameter = 14 cm) and dried at ambient conditions (T = 22 °C and RH = 53%) for 3 days, until the water was completely evaporated. The cast films were then dried overnight in a vacuum oven at 25 °C.

Free chitosan and nanocomposite films plasticized with glycerol were obtained by adding glycerol (25% (wt/wt) on solid CS) to the CS solution, while stirring for 20 min at 60 °C. Thereafter the procedure for the film preparation was identical to that described previously. The chitosan and nanocomposite films produced (average thickness 120 ± 5 μm) were respectively coded as follows:

- CS, CS/3MMT and CS/10MMT for unplasticized composite films;
- CS/GLY, CS/3MMT/GLY and CS/10MMT/GLY for films containing glycerol.

2.3. Characterization and measurements

2.3.1. X-ray analysis

The crystalline structure of chitosan polymer as well as the morphology of Na-MMT clay in the polymer was determined by WAXD measurements. An Anton Paar SAXSess diffractomer (40 kV, 50 mA) equipped with a Cu-Kα radiation (λ = 0.1542 nm) source and an image plate detector was used. The spectra were collected in transmission mode (i.e. a mode that allows the X-ray beam to move through the sample) by scanning the 2θ range from 1.5° to 40°. The samples were mounted with the casting surface orthogonal to the direction of the incident X-rays. All spectra were corrected only for the dark current and the empty holder background. In order to highlight the preferential orientation of the MMT platelets within the nanocomposites, WAXD spectra were also collected by samples that were rotated about 45° with respect to the incident X-rays.

2.3.2. Thermogravimetric analysis

The thermal stability of the nanocomposite films was evaluated by thermogravimetric analysis (TGA 2950, TA Instruments), in air, submitting the samples to a heating scan from 30 to 800 °C at a heating rate of 10 °C/min.

2.3.3. Water sorption kinetics

Chitosan films were cut in small pieces (1.2 cm × 1.2 cm), desiccated overnight under vacuum and weighed to determine their dry mass. The weighed films were placed in closed beakers containing 30 ml of water (pH = 7) and stored at T = 25 °C. The swelling kinetics were evaluated by periodically measuring the weight increment of the samples with respect to dry films with a balance accurate to 0.0001 g, after gently bottling the surface with a tissue, until equilibrium was reached. The water gain (W.G.) was calculated as follows:

$$\text{W.G.}(\%) = \frac{m_{\text{WetFilm}} - m_{\text{DryFilm}}}{m_{\text{DryFilm}}} \times 100 \quad (1)$$

where m_{WetFilm} and m_{DryFilm} are the weight of the wet and dry film, respectively.

2.3.4. Fourier transform infrared spectra

FTIR spectra were collected in transmission mode by using a Nicolet FTIR spectrophotometer in the range of 4000–400 cm^{-1} at a resolution of 4 cm^{-1}. Films having a thickness of 10–15 μm were prepared specifically for this analysis. All the obtained spectra were normalised for the respective thicknesses.

2.3.5. Water vapour permeability

The water vapour permeability was determined using the infrared sensor technique by means of a Permatran W 3/31 (Mocon, Germany). Samples with a surface area of 5 cm^2 were tested at 25 °C. Permeation tests were performed by setting the relative humidity at the downstream and upstream sides of the film to 0% and to 50% respectively. A flow rate of 100 ml/min of a nitrogen stream was used. Each test was carried out in duplicate.

2.3.6. Dynamic mechanical analysis

The dynamic mechanical properties of the composite films (strips 7 mm × 10 mm) were studied by means of a dynamic mechanical analyzer (DMA, Q8000, TA Instrument) in a tensile mode, from 20 to 250 °C at a frequency of 1 Hz and a heating rate of 3 °C/min. The samples were previously dried at 80 °C for 30 min in order to remove the free water. The glass transition was defined as the temperature at which tan δ reached the maximum value.

2.3.7. Mechanical properties

Tensile tests were performed with a Dynamometer (SANS, Model CMT4304), cutting the films into a dog-bone geometry according to the ASTM D-1708 procedure.

Nanoindentation tests were performed with a NanoTest Platform Two by Micro Materials Ltd., using a three-sided pyramidal (Berkovich) diamond indenter on specimens, with thickness of approximately 120 μm, which were stuck on flat aluminium stubs. In the tests, the indenter was pressed at a constant loading rate of 1 mN/s to a 3000 nm depth onto the surface of the film. The maximum load registered was then held constant for 60 s in order to monitor the creep behaviour of the material. Finally, the indenter was withdrawn from the surface, with same rate as in loading cycle, to 10% of the maximum load. At least 20 indents were performed on each sample at distances greater than 50 μm between each indentation. Reduced elastic moduli and hardness values have been obtained. Elastic modulus has been calculated using the following equation (Gregory & Spearing, 2005):

$$\frac{1}{E_r} = \frac{1-\nu^2}{E} + \frac{1-\nu_i^2}{E_i} \quad (2)$$

where E and ν are the elastic modulus and Poisson's ratio for the sample, respectively, and E_i and ν_i are the same quantities for the indenter. For the current analysis ν has been set equal to 0.35 (Krumova, Flores, Baltà Calleja, & Fakirov, 2002) while for diamond E_i has been set equal to 1141 GPa and (ν_i to 0.07 (Gregory & Spearing, 2005).

3. Results and discussion

3.1. XRD analysis

Fig. 1 reports the WAXD spectra for neat chitosan and nanocomposite films with two Na-MMT concentrations, with and without glycerol as plasticizer. Neat chitosan films show characteristic crystallinity peaks at $2\theta = 8°$, 11.2° and 18° as well as a broad peak corresponding to the amorphous structure at 23° (see the inset graph of the Fig. 1) (Wang et al., 2005). The crystalline structure of chitosan is strongly dependent on its processing treatment, as well as its origin and molecular constitution, such as degree of deacetylation and molecular weight (Rhim, Hong, Park, & Ng, 2006). However, the data reported in Fig. 1 show that the crystallinity of chitosan is slightly reduced by the addition of the Na-MMT clay and not affected by the presence of the glycerol plasticizer. The unmodified Na-MMT clay presents a distinctive diffraction peak at around $2\theta = 7.2°$, corresponding to a d_{001} spacing between the silicate platelets of about 1.2 nm. In Fig. 1 it can be observed that for chitosan/clay nanocomposites containing glycerol as plasticizer the Na-MMT diffraction peak shifts to 4.5° (i.e. d_{001} spacing equal to 1.8 nm corresponding to a thickness expansion of the original clay of about 50%). This shows that the chitosan macromolecules are able to intercalate the Na-MMT stacks. As for the chitosan/clay not containing glycerol, it is possible to detect a broaden shoulder, in the 2θ range between 5° and 7°, generally attributed both to poor intercalation (Wang et al., 2006) and mono-layered intercalation of chitosan macromolecules into Na-MMT stacks (Monvisade & Siriphannon, 2009). The obtained results indicate that the intercalation of chitosan chains within the silicate galleries takes place in different regimes of dispersions as well as to a different extent. The inter-platelet distance ranges from about 1.2 nm (related to the not-intercalated or poorly intercalated Na-MMT clay) up to 1.8 nm (related to Na-MMT clay intercalated through glycerol plasticizer assistance).

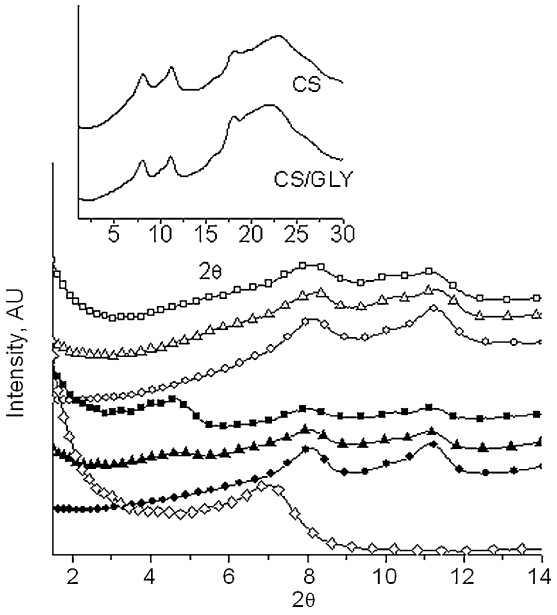

Fig. 1. XRD patterns of sodium montmorillonite (◊, Na-MMT), chitosan (○, CS), chitosan plasticized with glycerol (●, CS/GLY) and nanocomposite materials with different MMT concentration obtained by casting method, with (▲, CS/3MMT/GLY; ■, CS/10MMT/GLY) and without glycerol (△, CS/3MMT; □, CS/10MMT).

In order to better understand the structure of nanocomposites not containing glycerol, WAXD spectra of neat chitosan (CS) and nanocomposite with 10% (wt/wt) of Na-MMT (CS/10MMT), were collected by mounting the samples on the X-ray diffractometer holder with the casting surface both orthogonal and after rotation of 45° with respect to the incident X-rays. The results are shown in Fig. 2. The WAXD spectrum related to the 45° rotated sample containing 10% (wt/wt) of Na-MMT (coded Turned CS/10MMT) shows

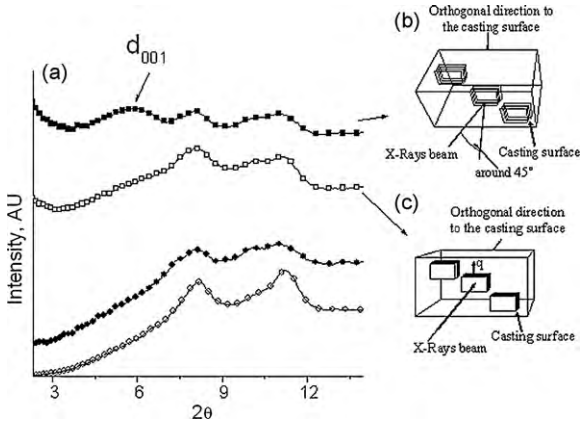

Fig. 2. (a) XRD patterns of CS/10MMT and neat chitosan collected with the specimens having the casting surface orthogonal and rotated of 45° with respect to the incident X-rays; (b) and (c) schematic representations of film orientations of nanocomposite having intercalated Na-MMT stacks with the platelets surface parallel to the casting surface. In (b) the scattering vector is not parallel to the platelets plane and then the diffraction is active, whereas in (c) the **q** vector is not active because its direction is parallel to the platelets plane. (○) CS, (●) turned CS, (□) CS/10MMT and (■) turned CS/10MMT.

a peak at $2\theta = 5.8^\circ$ corresponding to a *d*-spacing of 1.65 nm which is not present in the spectrum related to the sample mounted with the casting surface orthogonal to the incident X-rays. This may be assigned to the interlayer distance between silicate platelets of Na-MMT stacks poorly intercalated by chitosan macromolecules (i.e. the corresponding volume expansion of about 35% is lower than the volume expansion shown by the Na-MMT stacks in nanocomposites obtained with glycerol). The appearance of the peak through the rotation of the films suggests that the platelet surface of the MMT stacks is parallel to the casting surface. The same result has been observed for other MMT nanocomposites based on different polymers as already reported in the literature (Bafna, Beaucage, & Mirabella, 2003; Malwitz, Lin-Gibson, Hobble, Butler, & Schmidt, 2003). Varlot, Reynaud, Kloppfer, Vigier, and Varlet (2001) have shown that the diffracted intensity varies with the orientation of the MMT stacks inside the nanocomposites and it is highest when the stacks are orientated with the surface of the platelet parallel to the incident X-rays. The intensity decreases when a part of the stacks lays orthogonal to the direction of the incident X-rays. Thus, the results show that, for chitosan/clay nanocomposite films not containing glycerol, the Na-MMT stacks are preferentially orientated with the silicate platelets parallel to the surface of solution-casting film.

On the basis of XRD results, it can be summarized that chitosan/Na-MMT nanocomposites with intercalated clay structure, orientated or not, can been successfully prepared through a simple solution-intercalating mixing method. In particular during the casting process from acidic solution without the glycerol assistance, the MMT stacks tend to packing or flocculating preferentially with the platelet surface parallel to the casting surface. The formation of a flocculated structure may be attributed primary to the hydrogen-bonding interactions between the hydroxylated edge–edge of the silicate layers and the amino or hydroxyl functional groups of chitosan (Wang et al., 2006). In such case the intercalation by the migration of chitosan macromolecules into the silicate galleries may be difficult to be realized and this is confirmed by the WAXD results which indicate that only not-intercalated or poorly intercalated Na-MMT stacks are present in the composite films. The addition of glycerol plasticizer, on the other hand, reduces the extent of hydrogen-bonding interactions between chitosan and MMT edges by favouring preferential interactions between glycerol molecules and edge-MMT. This hinders the flocculation process and facilitates the intercalation, leaving the MMT stacks randomly orientated in the film.

Fig. 3 shows a schematic representation of the hypothesized Na-MMT stack orientation which occurs in the presence of glycerol plasticizer.

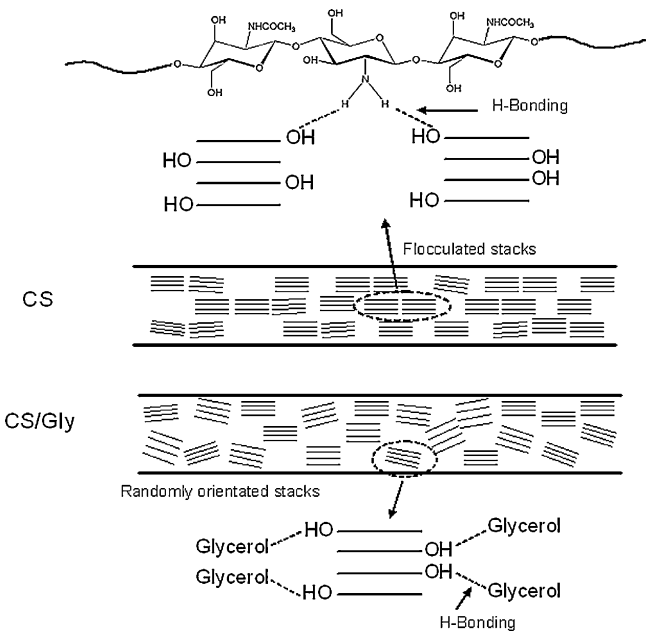

Fig. 3. XRD schematic representation of the Na-MMT stacks orientation as ruled by the presence of glycerol plasticizer.

3.2. Thermal stability

The thermal stability of chitosan and its nanocomposites was assessed by TGA analysis in air. Results obtained for films with and without plasticizer are reported in Fig. 4. Three steps of thermo-oxidative degradation are observed. The first one, in the temperature range 30–200 °C, is attributed to the loss of absorbed water. The second one, at around 270 °C, corresponds to the chemical degradation and deacetylation of chitosan (Wang et al., 2005, 2006). The third step, in the temperature range 450–600 °C, can be associated with the oxidative degradation of the carbonaceous residue formed during the second step. In the thermogravimetric analysis two parameters have been measured: respectively the temperature at which thermal degradation causes a loss of 20% and 50% weight. The results are summarized in Table1. Irrespective of the presence of glycerol, the degradation temperature of samples containing 10% (wt/wt) of Na-MMT on CS solid is improved by about 20 °C, probably due to the barrier provided by the platelets

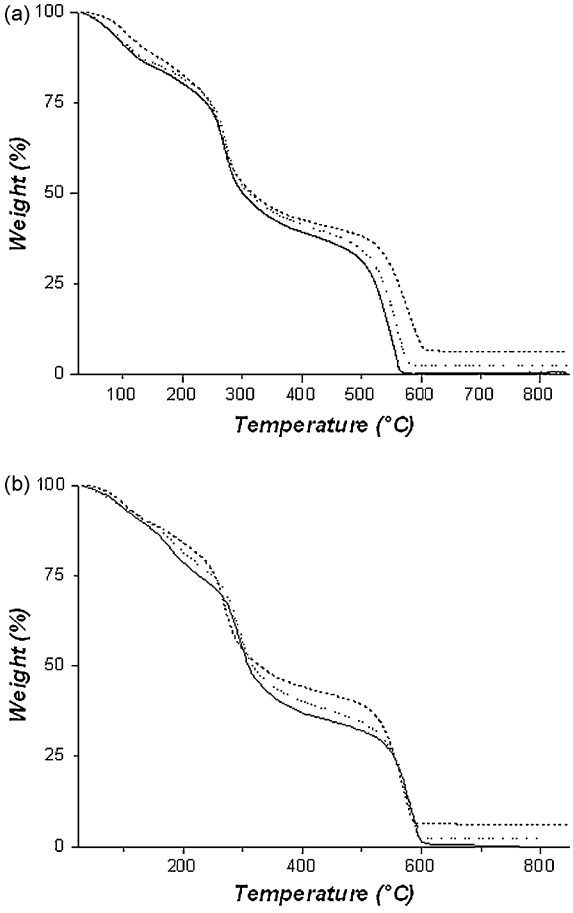

Fig. 4. TGA curves in air flow of (a) film not containing glycerol: (—) CS, (···) CS/3MMT and (- - -) CS/10MMT and (b) film containing glycerol: (—) CS/GLY, (···) CS/3MMT/GLY and (- - -) CS/10MMT/GLY.

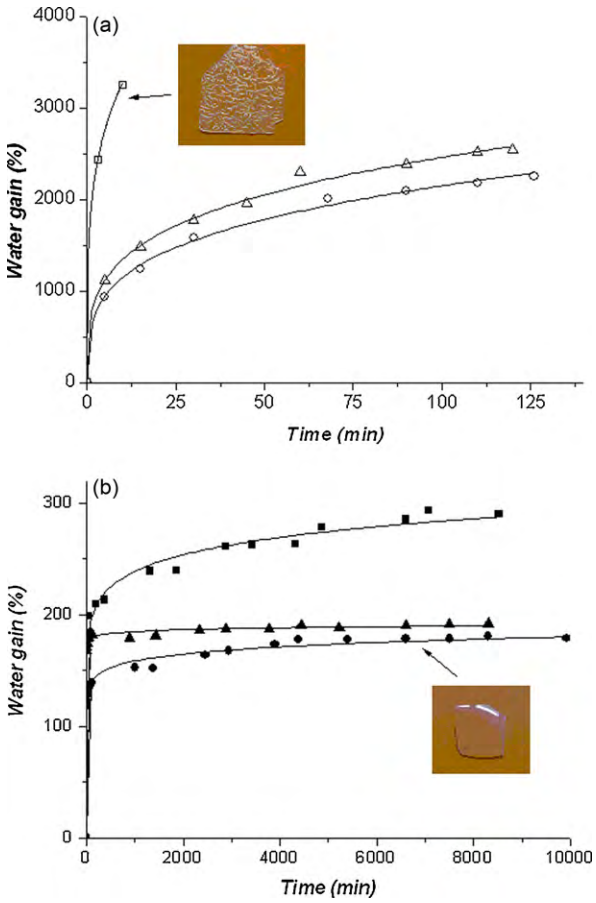

Fig. 5. Water sorption profiles at 25 °C and pH = 7 of (a) film not containing glycerol: (○) CS, (△) CS/3MMT and (□) CS/10MMT and (b) film containing glycerol: (●) CS/GLY, (▲) CS/3MMT/GLY and (■) CS/10MMT/GLY.

to the diffusion of oxygen (Wang et al., 2005). For nanocomposites containing glycerol, a further degradation step at $T \cong 250$ °C is observed, related to the loss of unbound glycerol, as indicated in Fig. 4. Furthermore, it can also be observed that the presence of glycerol plasticizer increases of about 20 °C the degradation temperature for the third step, irrespective of the presence or not of the nanoclay.

3.3. Water sorption kinetics

Water sorption profiles for films not containing glycerol are reported in Fig. 5a. The data show that for both chitosan and its nanocomposites, large amounts of water are rapidly absorbed into the films. In the first few minutes CS and CS/3MMT absorb almost 2000% water while in the case of CS/10MMT the uptake content can go up to 3000% of weight gain. All films swell and crumple before reaching equilibrium (see inset picture in Fig. 5a). After around 180 min for CS and after 20 min for CS/10MMT, the samples were completely dissolved. Fig. 5b reports water sorption profiles of neat chitosan and its nanocomposites obtained by adding glycerol as plasticizer to the casting procedure. It can be observed that they all reach the equilibrium values and that the amount of sorbed water is one order of magnitude less than films not containing glycerol. Thus the presence of glycerol confers a higher dimensional stability to the samples (see inset picture of Fig. 5b). This behaviour is most likely to be due both to the formation of the cross-link network induced by the hydrogen bonds between the chitosan and glycerol and to an enhanced intercalation of chitosan

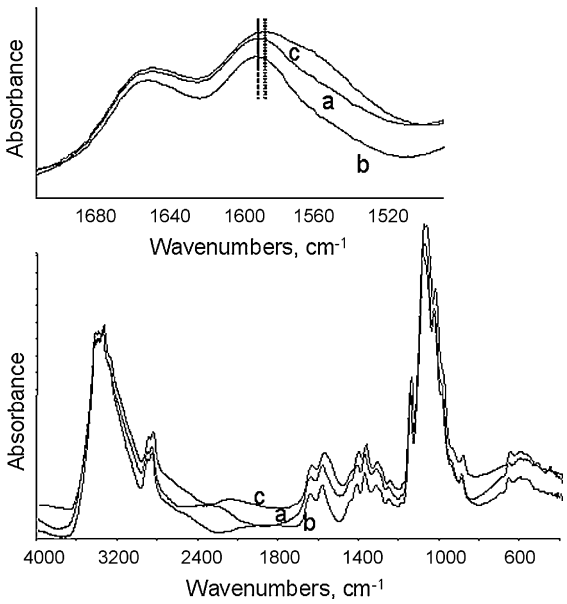

Fig. 6. FTIR spectra of (a) CS, (b) CS/GLY and (c) CS/3MMT. The inset graph shows the FTIR spectra in the wave numbers range between 1490 and 1710 cm^{-1}.

molecules into the silicate galleries, as confirmed by WAXD analysis.

3.4. FTIR analysis

FTIR spectroscopy analysis was performed to better understand the effects of glycerol and of Na-MMT filler on the structure of the chitosan nanocomposites. Fig. 6 reports FTIR spectra for both chitosan with and without glycerol plasticizer and the nanocomposite containing 3% (wt/wt) of Na-MMT without glycerol. All spectra exhibit the characteristic two strong bands of the amide groups at 1650 and 1590 cm^{-1} ascribed respectively to the C=O stretching and NH bending modes (Wang et al., 2005). The shoulder at approximately 1560 cm^{-1}, observed mainly for the samples not containing glycerol plasticizer, is assigned to the presence of $-NH_3^+$ $^-OOCCH_3$ interactions (Brown et al., 2001). This shoulder disappears when glycerol is added as plasticizer to the film formulation. The glycerol molecules are likely to displace the bound acetic acid from the chitosan macromolecules, thereby increasing the number of $-NH_2$ groups able to interact by H bonding with the available acceptor moieties (i.e. glycerol molecules, hydroxyl and ammine groups on the chitosan and hydroxyl groups on the edge of Na-MMT). The amide bands for chitosan with 3% (wt/wt) Na-MMT is slightly displaced towards low frequencies (i.e. the absorbance band of NH_2 vibration mode moves from 1588 to 1586 cm^{-1}) due to the H-bonding interaction between clay and chitosan, which facilitates the intercalation of the chitosan chains into the clay galleries (Chen & Zhang, 2006). FTIR spectroscopy results confirm that (1) acetic acid protonates the amine groups of chitosan to form chito-ammonium acetate, (2) glycerol molecules displace acetic acid in the formation of hydrogen bonding with amine groups and (3) Na-MMT clay interacts with chitosan macromolecules through hydrogen bonding involving the amide groups.

3.5. Water vapour permeability

The permeation characteristics of small molecular weight species, such as water vapour, was investigated to determine the combined effect of clays and glycerol plasticizer on the barrier properties of chitosan and its nanocomposites. Platelets clay is known to improve the barrier properties of polymers by creating a tortu-

Table 1
Summary of thermal, water permeability, mechanical properties for chitosan and its nanocomposites, with and without glycerol.

Sample	Temperature at 20% loss (°C)	Temperature at 50% loss (°C)	Tensile strength (MPa)	Extension at break (mm)	WVP $T = 25\,^{\circ}C$; $RH_{upstream} = 50\%$ (g/m s Pa)10^{-11}
CS/GLY	193	309	8.20 ± 2.93	13.65 ± 2.02	3.01
CS/3MMT/GLY	209	317	9.07 ± 2.37	9.60 ± 0.81	2.50
CS/10MMT/GLY	232	330	17.97 ± 0.80	7.98 ± 0.49	2.05
CS	202	301	26.01 ± 2.48	6.84 ± 1.57	2.38
CS/3MMT	216	312	26.95 ± 2.54	7.22 ± 0.60	2.14
CS/10MMT	220	317	32.59 ± 4.03	5.37 ± 0.19	1.16

ous path for the molecule diffusion. However, in the case of the hydrophilic chitosan matrix, the improvement of barrier properties could not be so prominent as expected for other polymers, due to the presence of polar group in clay (Tang et al., 2009). Table 1 reports the permeability data for chitosan and its nanocomposites, with and without glycerol. The presence of glycerol in both neat chitosan and its nanocomposites brings about an increase in water permeability. Moreover, these matrices show a decrease in water permeability with increasing of silicate loading. In particular, a higher decrease in permeability was observed in nanocomposites not containing glycerol. To better understand the experimental data, the principal factors affecting permeation have been taken into account. These include degree of crystallinity, level of dispersion and orientation of silicate platelets inside the matrix.

Despite the decrease of crystallinity degree evidenced by the XRD analysis, the permeability values of nanocomposites decrease. Thus, the observed reduction must be attributed exclusively to the presence and orientation of platelets.

The reduction of water permeability of about 30% and 50% respectively for CS/10MMT/GLY and CS/10MMT are in concordance with the identification of a preferential orientation of silicate platelets parallel to the surface of solution-casting film. The presence of silicate platelets in nanocomposite films leads to a reduction of water permeability, due to the tortuous path which hinders the diffusion of the permeant. In order to explain the difference in the extent of reduction between films with and without glycerol as plasticizer, it is important to take into account the fact that a higher reduction of permeability should be observed in such cases in which they are aligned and flocculated rather than randomly oriented, due to the high surface/height ratio of the platelets (Choudalakis & Gotsis, 2009). Thus, nanocomposites containing glycerol show a lower water permeability reduction due to the fact that the presence of glycerol plasticizer hinders the flocculation and leaves the MMT stacks randomly orientated in space (see Fig. 3).

3.6. Dynamic mechanical properties

Fig. 7a and b shows the plots of storage (E') and loss tangent ($\tan\delta$) as a function of temperature for neat chitosan and nanocomposites prepared with and without glycerol as plasticizer.

The $\tan\delta$ plot of neat chitosan without glycerol (see Fig. 7b) shows a prominent relaxation process at around 160 °C. This peak is attributed to the glass transition temperature of chitosan arising from the relaxation of two glucopyranose rings via the glucosidic oxygen and assisted by a cooperative hydrogen bonds reordering (Quijada-Garrido, Iglesias-Gonzalez, Mazon-Arechederra, & Barrales-Rienda, 2007). The shoulder at around 100 °C can be associated with the evaporation of residual water molecules. It is worth noting, however, that some reactions involving functional groups of chitosan, such as the decomposition of chitosonium groups to chitin, can take place in the range of temperature between 80 and 100 °C ($-NH_3^+\ ^-OOCCH_3 \Rightarrow -NH-OC-CH_3 + H_2O$) (Toffey, Samaranayake, Frazier, & Glasser, 1996). The presence of not-intercalated or poorly intercalated Na-MMT stacks, as revealed by WAXD analysis, does not significantly affect the thermo-mechanical behaviour of materials in terms of both Tg and height of the $\tan\delta$ peak.

As for the materials obtained using glycerol as plasticizer, the storage modulus increase with the Na-MMT contents in the glassy region. This increase suggests that the interactions between chitosan matrix and Na-MMT platelets are strong enough to allow an efficient load transfer between the matrix and the fillers. The glass transitions of the nanocomposites is slightly higher than that of neat chitosan and the area under the $\tan\delta$ curves is reduced, which is indication of a restriction to the relaxation movements of chitosan macromolecules probably due to the higher extent of the chitosan intercalation (as confirmed by WAXD analysis). The glass transition temperature decreases when glycerol is added, confirming its plasticizing effect on the chitosan polymeric network (Quijada-Garrido et al., 2007).

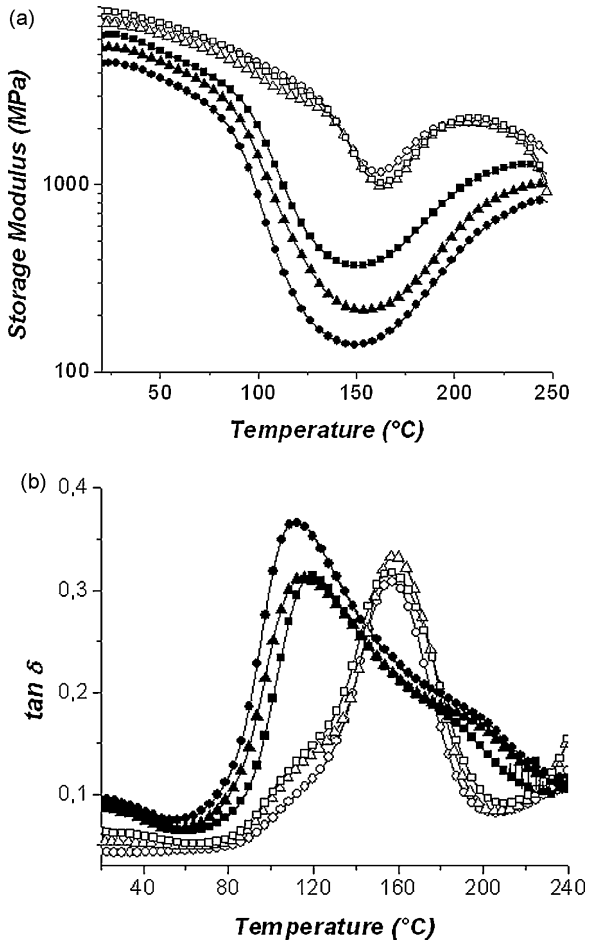

Fig. 7. DMA curves including storage modulus (a) and $\tan\delta$ (b) as a function of temperature for chitosan and its nanocomposites. (○) CS, (△) CS/3MMT and (□) CS/10MMT, (●) CS/GLY, (▲) CS/3MMT/GLY and (■) CS/10MMT/GLY.

Table 2
Elastic modulus and hardness from nanoindentation experiments of chitosan and its nanocomposites, with and without glycerol.

Sample	Modulus (GPa)	Hardness (GPa)
CS/GLY	1.70 ± 0.11	0.05 ± 0.01
CS/10MMT/GLY	3.67 ± 0.41	0.13 ± 0.02
CS	5.76 ± 0.29	0.18 ± 0.01
CS/10MMT	6.33 ± 0.89	0.23 ± 0.06

Regardless the preparation procedure, starting from 160 °C, the storage moduli increase with the temperature probably due to thermal transformations which occur in the bulk material. At temperature higher than 210 °C, the storage moduli of chitosan nanocomposites decreases because of thermal degradations of chitosan polymer, as confirmed by thermal gravimetric analysis.

3.7. Mechanical properties

The mechanical properties in tensile mode of nanocomposite films were investigated to complete the characterization of film behaviour. Table 1 reports the tensile strength and extension at break values of chitosan and its nanocomposites, with and without glycerol. It can be observed that the tensile strength values of neat chitosan and its nanocomposites containing glycerol are always lower than those of films without glycerol. Furthermore, a similar effect was also observed by Srinivasa et al. (2007) for films not containing glycerol, the presence of Na-MMT stacks does not significantly affect the tensile strength of the nanocomposites. In the case of films containing glycerol, on the other hand, the tensile strength of CS/10MMT/GLY is considerably higher than that of neat chitosan (CS/GLY). The presence of glycerol changes the hydrogen-bonding network within the material and allows both a better interaction between nanofiller and matrix and a higher extent of chitosan intercalation in Na-MMT clay.

The modulus and hardness values for chitosan and its nanocomposites, with and without glycerol plasticizer, determined by the nanoindentation technique, are shown in Table 2. It can be observed that both the moduli and hardness of the nanocomposites are higher than those of the unmodified systems. Furthermore, with a higher clay loading, as evidenced by the standard deviation of the reported results, the possibility of inhomogeneous distribution of clay is larger.

4. Conclusion

In this work chitosan-based nanocomposite films at different silicate loadings, with and without glycerol as plasticizer, were produced by solution-casting technique and characterized with particular regard to structural, thermal, barrier and mechanical properties. On the basis of obtained results it can been concluded that:

(1) Chitosan/Na-MMT nanocomposites exhibit an intercalated or intercalated/orientated structure of clays. In particular, the X-ray diffraction results show that in films without glycerol the MMT stacks lay with their platelet surface parallel to the casting surface. The presence of glycerol, on the other hand, enhances the chitosan intercalation in the silicate galleries and hinders the flocculation process, leaving the MMT stacks randomly orientated in the space.
(2) DMA, tensile and nanoindentation tests show that, as far as the effect of clay loading is concerned, mechanical properties of nanocomposite films without glycerol are not significantly affected by the presence of Na-MMT stacks. On the contrary, for nanocomposites containing glycerol, the mechanical properties are improved as clay loading increases. This is due to a combined effect of clays and plasticizer. Glycerol modifies the hydrogen-bonding network within the material and allows better interaction between filler and matrix, thus facilitating the stress transfer to the reinforcement phase and improving its mechanical properties.
(3) With respect to the barrier properties, a decrease of water permeability is obtained due to the presence of Na-MMT filler into the matrix. This is related to dispersion and orientation of silicate platelets inside the matrix, to the possible presence of polymer–clay interactions as well as to the interaction between chitosan matrix and glycerol. In particular, nanocomposites containing glycerol show a lower water permeability reduction (30%) due to plasticizing effect of glycerol which reduces the hydrogen interactions between chitosan and MMT, hinders the flocculation and leaves the MMT stacks randomly orientated in space. A higher reduction of permeability (50%) is obtained in chitosan films not containing glycerol due to the alignment and flocculation of MMT stacks.

Acknowledgements

The authors acknowledge Mr. Mario De Angioletti of Institute of Biomedical and Composite Materials-CNR for providing his useful support in nanoindentation experiments.

References

Bafna, A., Beaucage, G., & Mirabella, F. (2003). 3D Hierarchical orientation in polymer–clay nanocomposite films. *Polymer*, *44*, 1103–1115.
Brown, C. D., Kreilgaard, L., Nakakura, M., Caram-Lelham, N., Pettitb, D. K., Gombotzb, W. R., et al. (2001). Release of PEGylated granulocyte–macrophage colony-stimulating factor from chitosan/glycerol films. *Journal of Controlled Release*, *72*, 35–46.
Burgentzlè, D., Duchet, J., Gerard, J. F., Jupin, A., & Fillon, B. (2004). Solvent-based nanocomposite coatings. I. Dispersion of organophilic montmorillonite in organic solvents. *Journal of Colloid and Interface Science*, *278*, 26–39.
Chen, P., & Zhang, L. N. (2006). Interaction and properties of highly exfoliated soy protein/montmorillonite nanocomposites. *Biomacromolecules*, *7*, 1700–1706.
Choudalakis, G., & Gotsis, A. (2009). Permeability of polymer/clay nanocomposites: A review. *European Polymer Journal*, *45*, 967–984.
Correlo, V. M., Boesel, L. F., Bhattacharya, M., Mano, J. F., Neves, N. M., & Reis, R. L. (2005). Properties of melt processed chitosan and aliphatic polyester blends. *Materials Science and Engineering A*, *403*, 57–68.
Darder, M., Colilla, M., & Ruiz-Hitzky, E. (2003). Biopolymer–clay nanocomposites based on chitosan intercalated in montmorillonite. *Chemistry of Material*, *15*, 3774–3780.
Gregory, J. R., & Spearing, S. M. (2005). Nanoindentation of neat and in situ polymers in polymer-matrix composites. *Composites Science and Technology*, *65*, 595–607.
Gunster, E., Pestreli, D., Unlu, C. H., Atici, O., & Gungor, N. (2007). Synthesis and characterization of chitosan-MMT biocomposite systems. *Carbohydrate Polymers*, *67*, 358–365.
Krumova, M., Flores, A., Baltà Calleja, F. J., & Fakirov, S. (2002). Elastic properties of oriented polymers, blends and reinforced composites using microindentation technique. *Colloid Polymer Science*, *280*, 591–598.
Malwitz, M. M., Lin-Gibson, S., Hobble, E. K., Butler, P. D., & Schmidt, G. (2003). Orientation of platelets in multilayered polymer-nanocomposite films. *Journal Polymer Science Part B: Polymer Physics*, *41*, 3237–3248.
Monvisade, P., & Siriphannon, P. (2009). Chitosan intercalated montmorillonite: Preparation, characterization and cationic dye adsorption. *Applied Clay Science*, *47*, 427–431.
Olabarrietaa, I., Forsstrom, D., Gedde, U. W., & Hedenqvist, M. S. (2001). Transport properties of chitosan and whey blended with poly(1-caprolactone) assessed by standard permeability measurements and microcalorimetry. *Polymer*, *42*, 4401–4408.
Quijada-Garrido, I., Iglesias-Gonzalez, V., Mazon-Arechederra, J. M., & Barrales-Rienda, J. M. (2007). The role played by the interactions of small molecules with chitosan and their transition temperatures. Glass-forming liquids: 1,2,3-propantriol (glycerol). *Carbohydrate Polymers*, *68*, 173–186.
Rhim, J. W., Hong, S. I., Park, H. M., & Ng, P. K. W. (2006). Preparation and characterization of chitosan-based nanocomposite films with antimicrobial activity. *Journal Agricultural Food Chemistry*, *54*, 5814–5822.
Shanmugharaj, A. M., Rhee, K. Y., & Ryu, S. H. (2006). Influence of dispersing medium on grafting of aminopropyltriethoxysilane in swelling clay materials. *Journal of Colloid Interface Science*, *298*, 854–859.

Srinivasa, P. C., Ramesh, M. N., & Tharanathan, R. N. (2007). Effect of plasticizers and fatty acids on mechanical and permeability characteristics of chitosan films. *Food Hydrocolloids*, *21*, 1113–1122.

Tang, C., Chen, N., Zhang, Q., Wang, K., Fu, Q., & Zhang, X. (2009). Preparation and properties of chitosan nanocomposites with nanofillers of different dimensions. *Polymer Degradation and Stability*, *94*, 124–131.

Toffey, A., Samaranayake, G., Frazier, C. E., & Glasser, W. G. (1996). Chitin derivatives. Kinetics of the heat-induced conversion of chitosan to chitin. *Journal Applied Polymer Science*, *60*(1), 75–85.

Tual, C., Espuche, E., Escoubes, M., & Domard, A. (2000). Transport properties of chitosan membranes: Influence of crosslinking. *Journal Polymer Science Part B: Polymer Physics*, *38*, 1521–1529.

Varlot, K., Reynaud, E., Kloppfer, M. H., Vigier, G., & Varlet, J. (2001). Clay reinforced polyamide: preferential orientation of the montmorillonite sheets and the polyamide crystalline lamellae. *Journal Polymer Science Part B: Polymer Physics*, *39*, 1360–1370.

Wang, S. F., Shen, L., Tong, Y. J., Chen, L., Phang, I. Y., Lim, P. Q., et al. (2005). Biopolymer chitosan/montmorillonite nanocomposites: Preparation and characterization. *Polymer Degradation and Stability*, *90*, 123–131.

Wang, X., Du, Y., Yang, J., Wang, X., Shi, X., & Hu, Y. (2006). Preparation, characterization and antimicrobial activity of chitosan/layered silicate nanocomposites. *Polymer*, *47*, 6738–6744.

Xu, Y., Ren, X., & Hanna, M. A. (2006). Chitosan/clay nanocomposite film preparation and characterization. *Journal Applied Polymer Science*, *99*, 1684–1691.